

Cite this: *Chem. Sci.*, 2021, 12, 7073

All publication charges for this article have been paid for by the Royal Society of Chemistry

Received 23rd February 2021
Accepted 15th April 2021

DOI: 10.1039/d1sc01071a

rsc.li/chemical-science

Rapid amplitude-modulation of a diarylethene photoswitch: en route to contrast-enhanced fluorescence imaging†

Gaowa Naren,  ‡^a Wera Larsson,  ‡^a Carlos Benitez-Martin,  ^{bc} Shiming Li,  ^a Ezequiel Pérez-Inestrosa,  ^{bc} Bo Albinsson  ^{*a} and Joakim Andréasson  ^{*a}

A water soluble diarylethene (DAE) derivative that displays exceptionally intense fluorescence from the colorless open form has been synthesized and characterized using UV/vis spectroscopy and fluorescence microscopy. We show that the bright emission from the open form can be rapidly switched using amplitude modulated red light, that is, by light at wavelengths longer than those absorbed by the fluorescent species. This is highly appealing in any context where undesired background fluorescence disturbs the measurement, e.g., the autofluorescence commonly observed in fluorescence microscopy. We show that this scheme is conveniently applicable using lock-in detection, and that robust amplitude modulation of the probe fluorescence is indeed possible also in cell studies using fluorescence microscopy.

Introduction

Fluorescence microscopy is an indispensable tool for imaging applications in bio- and material sciences.^{1–6} Visualization of cellular components and the related processes is typically achieved using synthetic fluorescent probes that can be tagged to organelles/biomolecules with a high degree of specificity. While this approach allows for discrimination between fluorescent and non-fluorescent material, undesired autofluorescence from endogenous fluorophores inside the cells limits the signal-to-background ratio, which in turn decreases the contrast. When conventional fluorescent probes are used, amplitude modulation of the excitation light together with lock-in detection is of no use, as the background autofluorescence will oscillate with the same modulation frequency. Instead a tool is needed that enables amplitude modulation of the probe emission only, while keeping the autofluorescence intensity at a constant non-modulated level. The use of photochromic probes has been suggested for this purpose. Typically, the previously reported examples are demonstrated in bulk solution in organic solvents^{7–8} and with modulation frequencies of 1 Hz or lower.^{9–13} Limited bio-relevance and unpractically long acquisition times follows.

Moreover, the function of many of these molecular constructs relies on photo-controlled FRET reactions in multi-chromophoric constructs, implying extensive (synthetic) sample preparations.^{7–9,11–13} Additional attempts by Marriott and co-workers toward the realization of this scheme in a cellular environment utilizes a spiropyran photoswitch as the sole probe,^{10,14} implying a very low fluorescence quantum yield (around 0.01)¹⁵ and poor photostability. Also, the spiropyran is fluorescent in its colored isomeric form rather than in the colorless form. This situation presents several downsides in these contexts as the background fluorescence is much harder to separate from the probe fluorescence, requiring extensive data processing.

Instead, the optimal photoswitch for these purposes should be fluorescent in the colorless isomeric form. A high fluorescence quantum yield is, of course, also a requirement as is good photostability and water solubility. Here, we present the first example of a molecule that possesses all these features. We also show that lock-in detection is conveniently done at frequencies up to 200 Hz, and that the method is applicable in cell studies using fluorescence microscopy.

Results and discussion

The structure and the isomerization scheme for the asymmetric diarylethene^{16,17} (DAE asymmetric, Dasy) derivative used in this study are shown in Fig. 1.

The photoswitch exists in an open and a closed form referred to as Dasy(o) and Dasy(c), respectively. Dasy(o) absorbs almost exclusively in the UV region with its most redshifted absorption band centered at 351 nm in aqueous solution (see Fig. 2). Exposing Dasy(o) to UV light, here 365 nm, triggers isomerization to yield virtually 100% Dasy(c) at the photostationary state

^aChemistry and Chemical Engineering, Chemistry and Biochemistry, Chalmers University of Technology, 41296 Göteborg, Sweden. E-mail: a-son@chalmers.se; balb@chalmers.se

^bUniversidad de Málaga-IBIMA, Departamento de Química Orgánica, E-29071 Málaga, Spain

^cCentro Andaluz de Nanomedicina y Biotecnología (BIONAND), Parque Tecnológico de Andalucía, E-29590 Málaga, Spain

† Electronic supplementary information (ESI) available. See DOI: 10.1039/d1sc01071a

‡ Both authors contributed equally to the study.



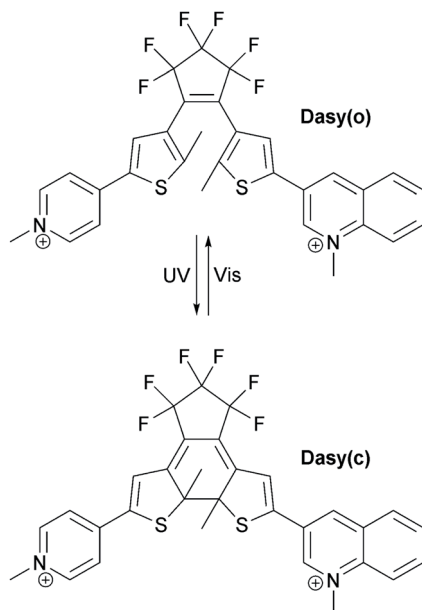


Fig. 1 Structure and isomerization scheme of the diarylethene derivative used in this study.

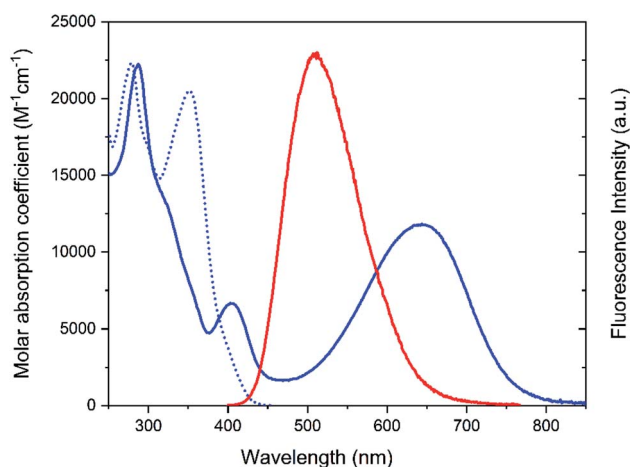


Fig. 2 Absorption and emission spectra of Dasy in aqueous solution. Dotted blue line: Dasy(o) absorption. Solid blue line: Dasy(c) absorption. Red line: Dasy(o) emission. Dasy(c) displays no detectable emission.

(PSS) with an isomerization quantum yield of 0.44. Dasy(c) displays absorption also in the visible region, manifested by a band with wavelength maximum at 644 nm. Dasy(c) is isomerized to yield 100% Dasy(o) by exposure to visible light, here 523 nm, with a quantum yield of 0.0033.

Left for 43 hours in the dark, Dasy(c) experiences *ca.* 15% decrease in absorption. We ascribe this change to the irreversible formation of a by-product rather than to the reversible isomerization to Dasy(o) (see Thermal stability and Fig. S1 in the ESI[†]).¹⁸

Dasy(c) is non-fluorescent, whereas Dasy(o) displays fluorescence emission centered around 511 nm in aqueous solution

with a fluorescence quantum yield and lifetime of 0.21 and 5.3 ns, respectively. A fluorescence quantum yield of 0.21 is extremely high for the open isomer of a DAE derivative. The one reported example with a higher number comes with the downside that it is only poorly enriched in the closed isomer upon UV isomerization, implying that “on-off” switching of the emission cannot be achieved.¹⁹ Considering also that there is currently no other class of photochromic molecules with intrinsically high fluorescence quantum yield in the colorless form, it is obvious that Dasy is a “par excellence” fluorescent photoswitch.

Typically, fluorescence modulation using photoswitches implies light-induced toggling between the two PSS induced by exposure to UV and visible light, respectively.^{20–32} The fluorescence intensities are recorded after isomerization to each state. Most often, this approach results in binary “on-off” switching of the fluorescence. This scheme is, of course, applicable to Dasy too and the resulting fluorescence changes are shown in Fig. S2 in the ESI.[†] Fluorescence switching is by no means restricted to this binary situation as the two extreme points do not have to be defined by the two pure PSS that result after UV and visible light exposure, respectively. In our approach, Dasy is initially in the fluorescent open Dasy(o) isomeric form. Exposure to continuous UV light at 365 nm results in emission of intense fluorescence as well as UV-induced isomerization to the closed non-fluorescent isomer Dasy(c). If this process continues until the PSS is reached, the sample is converted to virtually 100% Dasy(c) and no fluorescence is observed. If the sample at this point is exposed also to red light (triggering isomerization from Dasy(c) to Dasy(o)) the fluorescence will recover with the same rate as the establishment of the new PSS induced by simultaneous exposure to UV and red light, referred to as k_{obs} . Switching off the red light leads again to a gradual decrease of the fluorescence intensity, reflecting the UV-induced

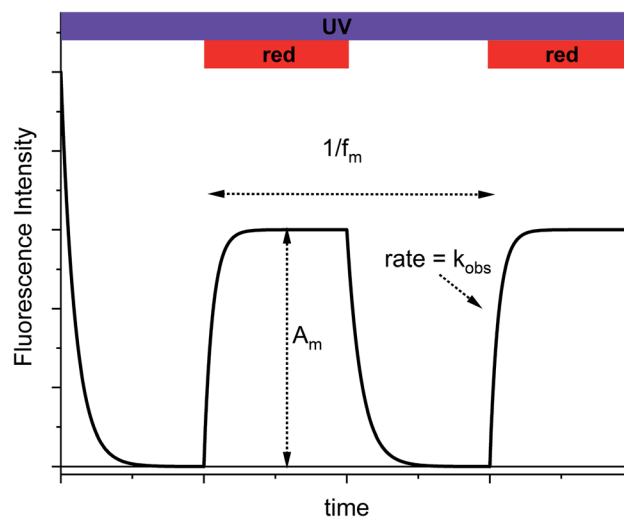


Fig. 3 Schematic depiction of the switching scheme applied in this study. A_m = modulation amplitude, f_m = modulation frequency, k_{obs} = rate constant for establishment of the PSS induced by simultaneous exposure to UV and red light.



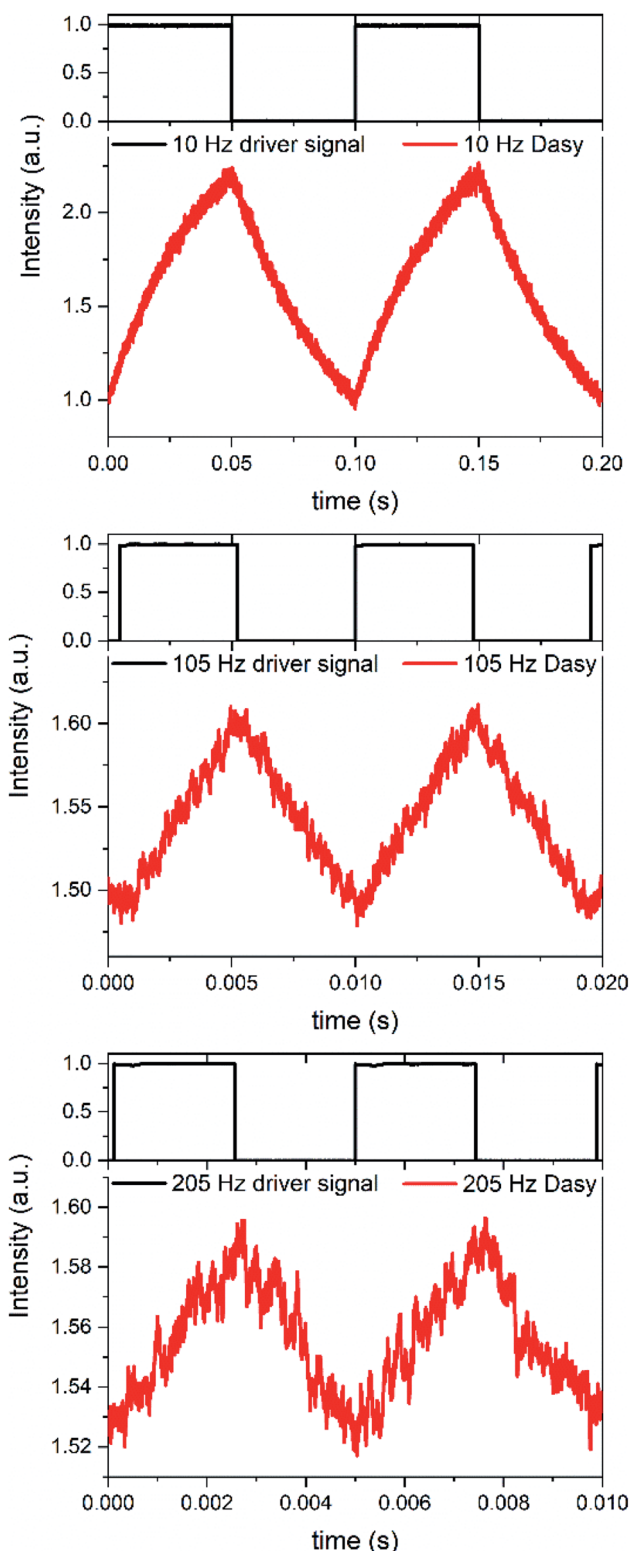


Fig. 4 Amplitude modulated fluorescence of Dasy in aqueous solution at varying modulation frequencies. The driver signal (black lines) controls the intensity of the laser diode at 660 nm. The fluorescence intensity from Dasy simultaneously exposed to continuous light at 365 nm and amplitude modulated light at 660 nm is shown in red. Modulation frequencies: 10 Hz (top), 105 Hz (middle), and 205 Hz (bottom).

isomerization to non-fluorescent Dasy(c). This switching scheme is schematically shown in Fig. 3 and illustrates the appealing idea that the fluorescence intensity of a fluorophore can be controlled by exposure to light at wavelengths much longer than those covered by the absorption spectrum of the fluorescent species.

If the on-off toggling of the red light occurs faster, equivalent to increasing the modulation frequency f_m , there is not time for the sample to fully isomerize between the two PSS. This applies when $f_m > k_{obs}$ and implies that the difference between the maximum and the minimum fluorescence intensities, referred to as the modulation amplitude A_m , will decrease. This is experimentally illustrated in Fig. 4 for an aqueous solution of Dasy at *ca.* 20 μM , continuous UV light at 365 nm (~ 30 mW) and square-wave modulated red light at 660 nm (~ 40 mW) at different frequencies.

It is clearly observed that A_m decreases with increasing f_m . Although estimation of A_m is possible from the crude signal up to $f_m = 205$ Hz, lock-in detection facilitates the separation of the ac-component A_m from the underlying dc-component substantially. A_m was plotted vs. f_m at 18 frequencies in the interval between 0.1 Hz and 205 Hz and it is very encouraging to note that the resulting plot is well described using a theoretical model for this situation, based on single exponential relaxation to the PSS (see Modulation amplitude A_m vs. modulation frequency f_m , and Fig. S3 and S4 in the ESI[†]).

As indicated above, lock-in detection allows for facile separation of an ac-component from an underlying dc-component. This is particularly appealing in situations where the probe fluorescence is obscured by undesired background fluorescence, *e.g.*, in fluorescence microscopy and cell studies. This

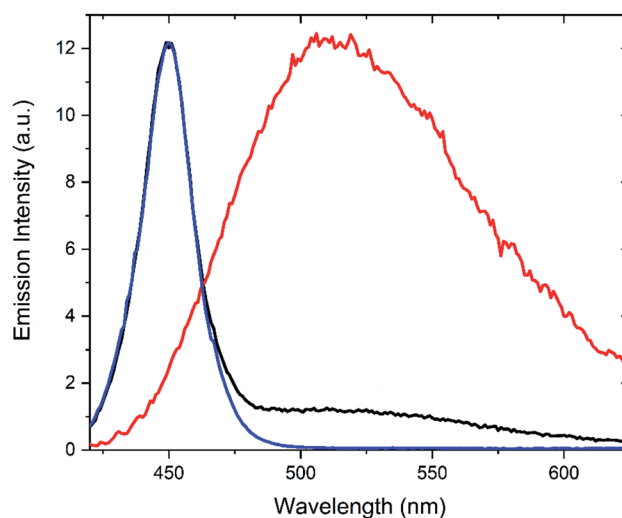


Fig. 5 Normalized emission spectra corresponding to the following situations: spectral profile of the light source with maximum at 450 nm (blue), overall spectrum of Dasy fluorescence + 450 nm light source recorded using conventional steady-state methodology (black), and amplitude-modulated fluorescence of Dasy (continuous irradiation at 365 nm and amplitude modulated light at 660 nm) + 450 nm light source (red). Acquisition times for all spectra were approximately four minutes.



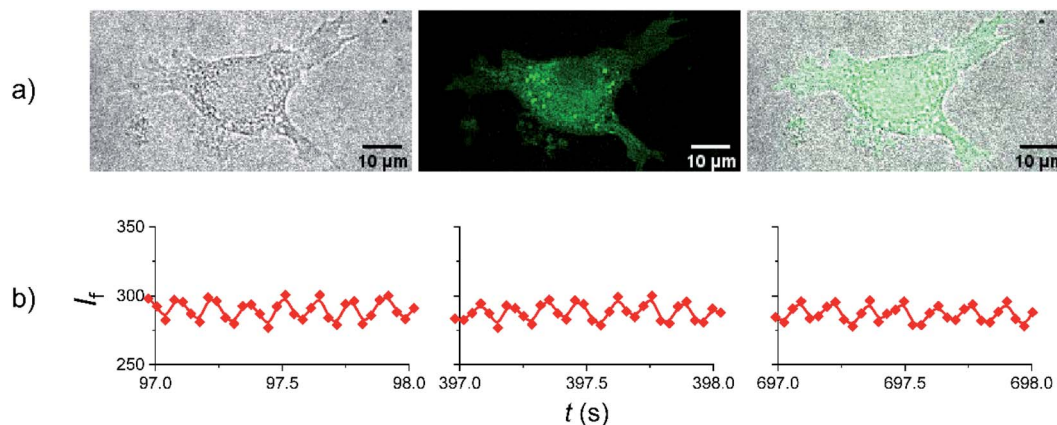


Fig. 6 (a) Fluorescence imaging of Dasy within a L929 cell. From left to right: brightfield, fluorescence emission, and merge. (b) Zoom-ins of the amplitude-modulated fluorescence in three different time windows. The 405 nm and 633 nm lines from the microscope were used to trigger the fluorescence amplitude modulations and the fluorescence was recorded in the green spectral region. See text for additional details.

procedure is referred to as optical lock-in detection (OLID).¹⁰ To investigate if the Dasy fluorescence could be filtered out from an intense background emission, the following experiment was undertaken: an aqueous solution of Dasy(o) was prepared at *ca.* 20 μM . The sample was excited continuously at 365 nm and the emission spectrum was recorded while the detector was simultaneously irradiated with a 450 nm light source (the spectral distribution of the light source is shown in Fig. 5, blue line) to represent the background. The resulting spectrum is shown in black in Fig. 5. It is clear that the dominating emission is the 450 nm light source. Please note that in this experiment, the red light at 660 nm was off at all times, and the detector signal was not filtered using lock-in detection. Next, the experiment was repeated, but this time the 660 nm red light was modulated at 10 Hz, and the detector signal was filtered by a lock-in amplifier set to the same frequency. The red line in Fig. 5 resulted. Here, the spectral signature from the 450 nm light source is entirely suppressed, and the recorded spectrum is instead in perfect agreement with that of Dasy(o) alone (*cf.* Fig. 2). This clearly shows that amplitude modulation using a red light-source and lock-in detection enables the total suppression of a dominating undesired background emission. The underlying explanation is that the only emission that is phase modulated and picked up by the lock-in amplifier is the fluorescence from Dasy(o). This corresponds to the very common situation of a background fluorescence from endogenous fluorophores absorbing the UV light (365 nm) but not the modulated red light at 660 nm.

Having established that amplitude modulated fluorescence from Dasy is achievable “in the cuvette” using conventional spectroscopic equipment, we opted for experiments to prove that the switching scheme can be applied also in fluorescence imaging inside cells. L929 cells were treated overnight with a complete medium solution containing Dasy(o) at a concentration of 100 μM and fixed before the microscopy experiments (see Materials and methods in the ESI† for full description of the cell culture and cell treatment). Judging by the fluorescence distribution from inside the cell shown in Fig. 6a it is apparent

that Dasy(o) does not display a specific subcellular localization. Instead, the fluorescence is spread throughout the cytoplasm. This observation is not unexpected due to the absence of targeting groups in the Dasy structure. It is also seen that Dasy does not seem to accumulate in the cellular nucleus, as further illustrated in Fig. S6 in the ESI.†

Please note that the images shown in Fig. 6a were recorded using conventional fluorescence imaging. In the subsequent amplitude modulation experiment the 405 nm and 633 nm laser lines were used to trigger the closing and the opening reactions, respectively. The 405 nm laser line also served as excitation for emission readout. A sequential scan program that yields an apparent modulation frequency of 7.4 Hz for the 633 nm light was employed, containing four scans or images per frame. The first two scans were acquired with simultaneous irradiation at 405 nm and 633 nm, whereas in the last two scans only 405 nm irradiation was employed. The results are displayed in Fig. 6b. Further details are described in the ESI (Materials and methods, Amplitude modulation of Dasy in fixed cells using fluorescence microscopy, and Fig. S5†). Zoom-ins of selected time windows spaced by 300 s are shown to emphasize the 7.4 Hz amplitude modulation (ac component) and the excellent photostability. Thus, the ability of Dasy to display amplitude modulated fluorescence within a biological environment is not only proved but is also ensured through the demonstrated fatigue resistance. Note that the extensive monitoring period of around 700 s is not required for the overall collection of amplitude modulated Dasy fluorescence, which would have implied unpractically long acquisition times. Instead, the chosen irradiation scheme serves as a control to the said photostability.

Conclusions

Judging from the fluorescence experiments performed both in the cuvette and in a cellular milieu using a microscope, we conclude that Dasy is a prime candidate for contrast-enhanced fluorescence imaging. We base this notion on the outstanding properties that this photoswitch presents, such as the water



solubility, exceptionally high fluorescence quantum yield, virtually 100% enrichment in both photostationary states (UV- and visible light induced), excellent photo- and thermal stability, redshifted absorption spectra, and rapid switching capabilities. For the demonstrated function *per se*, the key observation is that the photoswitch is highly fluorescent in the colorless open isomer. This should be contrasted to derivatives from other classes of photochromic compounds where the only emission originates from the weakly fluorescent colored forms, and also to other diarylethene structures (sulfone derivatives) with high brightness that fluoresces mainly in the closed colored isomer.³¹ A fluorescent colorless form implies that light at longer wavelengths than those absorbed by the fluorescent species can be used to influence the emission intensity in a controlled manner. Specifically, here we use light at 633 nm or 660 nm to induce amplitude modulation of the fluorescence centered at 511 nm. All endogenous material in the cell that contributes to undesired background fluorescence in the visible region, as well as scattered light, are totally unaffected by light at these wavelengths. This is why we efficiently can filter out the amplitude modulated Dasy-fluorescence from the constant background. Note that this scheme is not applicable using other frequently employed photoswitches that almost exclusively presents fluorescence in the colored isomeric form, such as the spiropyran used in the previously reported cell studies.^{10,14} We would also like to emphasize that the absorption band of the fluorescent form Dasy(o) extends beyond 400 nm as opposed to most other photochromic switches where the colorization reaction has to be triggered at 365 nm or shorter. This implies conveniently that the line at 405 nm can be used in the microscopy experiments and also a reduced phototoxicity.

Not only do we demonstrate amplitude modulation, but we also do it at frequencies that are orders of magnitude higher compared to the typical previous demonstrations (205 Hz vs. < 1 Hz) while maintaining amplitude modulation sufficiently large to be detected from the crude signal and, of course, also conveniently using lock-in detection. Thus, the acquisition times are dramatically shortened compared to approaches requiring modulation frequencies of 1 Hz or lower. In addition to the typical benefits of shorter acquisition times, it also enables live cell studies that would be impossible at lower frequencies.

Finally, the ultimate performance of Dasy in fluorescence imaging cannot be shown without lock-in interfaced detection in the microscope as no contrast-enhanced images can be recorded in its absence. This is, however, a matter of technical nature and does not devalue the excellent performance of Dasy demonstrated in the amplitude modulated proof-of-principle studies described above. Although the examples are very scarce,¹⁴ fluorescence imaging using OLID at modulation frequencies higher than 100 Hz has been demonstrated using a spiropyran photoswitch, clearly showing the potential of this technique. Considering the outstanding photophysical properties of Dasy discussed above, we believe that this novel photoswitch will substantially enhance the performance of OLID high-contrast imaging,³³ and may open up new research avenues that have not been available before.

Author contributions

J. A. conceptualization, formal analysis, funding acquisition, methodology, project administration, supervision, writing – original draft. B. A. conceptualization, formal analysis, funding acquisition, methodology, project administration, supervision. G. N. and W. L. formal analysis, investigation, methodology, visualization, writing – original draft. S.-M. L. investigation, methodology. C. B.-M. and E. P.-I. formal analysis, investigation, methodology, visualization. G. N. and W. L. contributed equally to this study.

Conflicts of interest

There are no conflicts of interest to declare.

Acknowledgements

J. A. and B. A. acknowledge financial support from the Swedish Research Council VR (Grant # 2016-0360 and Grant # 2018-03998, respectively). E. P.-I. acknowledges the Spanish Ministry for Science, Innovation, and Universities (RD16/0006/0012, PCI2019-111825-2, and PID2019-104293GB-I00), Universidad de Málaga-Junta de Andalucía (UMA18-FEDERJA-007), and FEDER. C. B.-M. is grateful for a FPU fellowship (FPU16/02516). The authors thank Dr Tamara Pace and Dr Vilhelm Müller for participating in the initial studies of Dasy.

Notes and references

- B. C. Chen, W. R. Legant, K. Wang, L. Shao, D. E. Milkie, M. W. Davidson, C. Janetopoulos, X. F. S. Wu, J. A. Hammer, Z. Liu, B. P. English, Y. Mimori-Kiyosue, D. P. Romero, A. T. Ritter, J. Lippincott-Schwartz, L. Fritz-Laylin, R. D. Mullins, D. M. Mitchell, J. N. Bembenek, A. C. Reymann, R. Bohme, S. W. Grill, J. T. Wang, G. Seydoux, U. S. Tulu, D. P. Kiehart and E. Betzig, *Science*, 2014, **346**, 1257998.
- F. Helmchen and W. Denk, *Nat. Methods*, 2005, **2**, 932–940.
- B. Huang, M. Bates and X. W. Zhuang, *Annu. Rev. Biochem.*, 2009, **78**, 993–1016.
- J. W. Lichtman and J. A. Conchello, *Nat. Methods*, 2005, **2**, 910–919.
- R. M. Power and J. Huisken, *Nat. Methods*, 2017, **14**, 360–373.
- S. J. Sahl, S. W. Hell and S. Jakobs, *Nat. Rev. Mol. Cell Biol.*, 2017, **18**, 685–701.
- G. Copley, J. G. Gillmore, J. Crisman, G. Kodis, C. L. Gray, B. R. Cherry, B. D. Sherman, P. A. Liddell, M. M. Paquette, L. Kelbauskas, N. L. Frank, A. L. Moore, T. A. Moore and D. Gust, *J. Am. Chem. Soc.*, 2014, **136**, 11994–12003.
- A. E. Keirstead, J. W. Bridgewater, Y. Terazono, G. Kodis, S. Straight, P. A. Liddell, A. L. Moore, T. A. Moore and D. Gust, *J. Am. Chem. Soc.*, 2010, **132**, 6588–6595.
- S. Mao, R. K. P. Benninger, Y. L. Yan, C. Petchprayoon, D. Jackson, C. J. Easley, D. W. Piston and G. Marriott, *Biophys. J.*, 2008, **94**, 4515–4524.



- 10 G. Marriott, S. Mao, T. Sakata, J. Ran, D. K. Jackson, C. Petchprayoon, T. J. Gomez, E. Warp, O. Tulyathan, H. L. Aaron, E. Y. Isacoff and Y. L. Yan, *Proc. Natl. Acad. Sci. U. S. A.*, 2008, **105**, 17789–17794.
- 11 C. Petchprayoon, Y. L. Yan, S. Mao and G. Marriott, *Bioorg. Med. Chem.*, 2011, **19**, 1030–1040.
- 12 Z. Y. Tian, W. W. Wu, W. Wan and A. D. Q. Li, *J. Am. Chem. Soc.*, 2011, **133**, 16092–16100.
- 13 Y. L. Yan, C. Petchprayoon, S. Mao and G. Marriott, *Philos. Trans. R. Soc., B*, 2013, 368.
- 14 L. X. Wu, Y. R. Dai, X. L. Jiang, C. Petchprayoon, J. E. Lee, T. Jiang, Y. L. Yan and G. Marriott, *Plos One*, 2013, **8**, e64738.
- 15 J. R. Nilsson, S. M. Li, B. Önfelt and J. Andréasson, *Chem. Commun.*, 2011, **47**, 11020–11022.
- 16 M. Irie, *Chem. Rev.*, 2000, **100**, 1685–1716.
- 17 M. Irie, T. Fukaminato, K. Matsuda and S. Kobatake, *Chem. Rev.*, 2014, **114**, 12174–12277.
- 18 M. Irie, T. Lifka, K. Uchida, S. Kobatake and Y. Shindo, *Chem. Commun.*, 1999, 747–748, DOI: 10.1039/a809410a.
- 19 K. Shibata, L. Kuroki, T. Fukaminato and M. Irie, *Chem. Lett.*, 2008, **37**, 832–833.
- 20 J. Andréasson, U. Pischel, S. D. Straight, T. A. Moore, A. L. Moore and D. Gust, *J. Am. Chem. Soc.*, 2011, **133**, 11641–11648.
- 21 J. Andréasson, S. D. Straight, T. A. Moore, A. L. Moore and D. Gust, *J. Am. Chem. Soc.*, 2008, **130**, 11122–11128.
- 22 C. Benitez-Martin, S. M. Li, A. Dominguez-Alfaro, F. Najera, E. Perez-Inestrosa, U. Pischel and J. Andréasson, *J. Am. Chem. Soc.*, 2020, **142**, 14854–14858.
- 23 L. Giordano, T. M. Jovin, M. Irie and E. A. Jares-Erijman, *J. Am. Chem. Soc.*, 2002, **124**, 7481–7489.
- 24 A. J. Myles, B. Gorodetsky and N. R. Branda, *Adv. Mater.*, 2004, **16**, 922–925.
- 25 F. M. Raymo and M. Tomasulo, *Chem. Soc. Rev.*, 2005, **34**, 327–336.
- 26 F. M. Raymo and M. Tomasulo, *J. Phys. Chem. A*, 2005, **109**, 7343–7352.
- 27 P. Remon, M. Bälter, S. M. Li, J. Andréasson and U. Pischel, *J. Am. Chem. Soc.*, 2011, **133**, 20742–20745.
- 28 L. Song, E. A. Jares-Erijman and T. M. Jovin, *J. Photochem. Photobiol., A*, 2002, **150**, 177–185.
- 29 L. W. Song, Y. H. Yang, Q. Zhang, H. Tian and W. H. Zhu, *J. Phys. Chem. B*, 2011, **115**, 14648–14658.
- 30 S. D. Straight, J. Andréasson, G. Kodis, S. Bandyopadhyay, R. H. Mitchell, T. A. Moore, A. L. Moore and D. Gust, *J. Am. Chem. Soc.*, 2005, **127**, 9403–9409.
- 31 K. Uno, H. Niikura, M. Morimoto, Y. Ishibashi, H. Miyasaka and M. Irie, *J. Am. Chem. Soc.*, 2011, **133**, 13558–13564.
- 32 H. Zhao, U. Al-Atar, T. C. S. Pace, C. Bohne and N. R. Branda, *J. Photochem. Photobiol., A*, 2008, **200**, 74–82.
- 33 Y. L. Yan, M. E. Marriott, C. Petchprayoon and G. Marriott, *Biochem. J.*, 2011, **433**, 411–422.

